

A Feasibility Study of Axial Injection Method for the CYRIC 680-Cyclotron

著者	Honma T., Fujioka M., Goto A., Shinozuka T.
journal or publication title	CYRIC annual report
volume	1992
page range	51-55
year	1992
URL	http://hdl.handle.net/10097/49691

I. 11. A Feasibility Study of Axial Injection Method for the CYRIC 680-Cyclotron

Honma T., Fujioka M., Goto A. and Shinozuka T.*

*Cyclotron and Radioisotope Center, Tohoku University
The Institute of Physical and Chemical Research**

Introduction

A new idea of an off-axis axial injection method has been studied numerically for the CYRIC 680 AVF cyclotron. Basic notion of the method and some calculational results are presented. In the previous studies of particle orbit behaviors in the 680-cyclotron central region¹⁾, we knew that axially injected beams have large betatron amplitudes in the both radial and vertical planes in comparison with the particles from the internal ion source. The expected amplitude, for example, in the vertical plane was about ± 10 mm for the starting condition of (0 mm, 100 mrad) in the upright phase ellipse for proton injection energy of 10 keV. Hence the vertical acceptance in the central region is mainly restricted by the dee aperture of 26 mm. Therefore the maximum allowable divergence of the injected particle should not exceed ± 100 mrad.

On the other hand, an electrostatic mirror, which would have a 23 mm outer diameter of the electrode housing was selected as an inflector due to the small space in the central region. We further studied the beam orbit through this mirror, and found that it should be positioned off-axis from the axial hole center. The optimum off-axis distance of the beam at the entrance of mirror was found to be about 15 mm as shown in Fig.1. In this report we show that the displacement of the beam mentioned above is indeed possible. We assume that inside the axial hole the residual magnetic field has the rotational symmetry. It is noted that the beam will be bent toward the field axis if the initial beam direction is off-axis and parallel to the axis of symmetry of the magnetic field. This can be compensated by placing correction elements such as electrostatic deflecting plates in the beam line.

Basic principle

The equation of motion of a particle of charge q and mass m in a combined electric and magnetic fields is ;

$$\dot{\vec{p}} = q \cdot \vec{E} + q \cdot (\vec{v} \times \vec{B}), \quad (1)$$

where the dot indicate differentiation with respect to time. In cylindrical coordinates (r, θ, z) the component p_θ , which act on the particle as a rotating force in the axially symmetric magnetic field, is represented as ;

$$\dot{p}_\theta = q \cdot E_\theta (r, z) + \frac{1}{m} \{ p_r \cdot (-p_\theta / r - q B_z (r, z)) + q \cdot B_r (r, z) \cdot p_z \}, \quad (2)$$

where the transversal momentum components p_r and p_θ can be considered to be negligibly small in comparison with the longitudinal momentum p_z ; on the other hand the radial magnetic field component $B_r (r, z)$ can not be ignored due to the condition of the off-axis injection. Then the force component \dot{p}_θ can be reduced by making a condition in eq.(2) as ;

$$E_\theta (r, z) = -v_z \cdot B_r (r, z), \quad (3)$$

where $B_r (r, z)$ is calculated by using the measured magnetic field $B_z (0, z)$ along the axial hole, and is represented as ;

$$B_r (r, z) = -\frac{1}{2} B_z' (0, z) \cdot r + \frac{1}{16} B_z''' (0, z) \cdot r^3, \quad (4)$$

The measured field $B_z (0, z)$ inside the axial hole for various magnetic excitations are shown in Fig. 2 and the calculated $B_r (r, z)$ at an excitation current of 500 A is plotted in Fig. 3. In eq.(3) the problem is how to produce such an electric field in the axial hole.

Electric field

The characteristics of the electric field which satisfy the relation of eq.(3) is; the strength of the field component $E_\theta (r, z)$ be proportional to the radial magnetic field component $B_r (r, z)$ and increase with the radial distance from the hole axis. Such an "ideal" electric field, however, can not be created for a finite region of the space due to the basic relation of Maxwell's equations, $\text{div } \vec{E} = 0$ and $\text{rot } \vec{E} = 0$. Then it is necessary to substitute the ideal field by a practical one, which looks like a quadrupole field produced by a pair of electrodes. Schematic drawing of the electrode assembly is illustrated in Fig. 4. Three dimensional electric field with these electrodes was calculated by using the code RELAX3D²⁾. Examples of the field characteristics are shown in Fig.5

Orbit calculation

A computer code was developed to calculate the particle trajectory in the electric and magnetic fields with time as the independent variable. The code has been used to compute the particle trajectories not only in the axial hole but also inside the mirror. The ion of proton beam for 10 kV injection voltage and the central field value of $B_0 = 9.45$ kG have been selected to study the particle trajectories from the starting point (S.P.) at $z = -14$ cm down to the cyclotron median plane (M.P) at $z = 0$.

In the first place, the particle trajectories have been calculated for the ideal electric field for some test particles contained in the emittance of 300π mm - mrad upright ellipse. The results are shown in Fig. 6 as projected onto the X-Y median plane, as well as the phase spaces at S. P. and at M. P. Small circles are orbits of the particles projected onto the median plane. This circular motion arises from the fact that we can not always keep $p_\theta = 0$ because at S.P. the momentum components of p_r and p_θ are not always zero.

In the second place, particle trajectories have been calculated under the practical electric field produced by the suitable set of electrodes as described in sec. 3. In this case the initial beam conditions at S.P. were replaced by a more realistic ones having Gaussian beam profiles in the X and Y planes with both the emittance of 300π mm - mrad ($\pm 2 \sigma$).

Finally the study has been extended to calculate the particle trajectories through the mirror inflector. Here the parameters of the mirror are taken following the Bellomo's notation³⁾ as ;

$$\frac{1}{2} \tau_\theta^2 = \tan^2 \alpha (1 - \cos \tau_\theta) \quad (5)$$

where τ_θ is the transit time inside the mirror and α is the mirror angle of 46 deg. The result of calculation for 15 mm off-axis injection is shown in Fig. 7. The trajectories for 100 particles were calculated from S.P. until the mirror exit; see Fig. 7. Other details are given in the figures.

Conclusion

As described above the studies have been made under the condition roughly satisfying eq.(3). They show that an axial injection may be possible for the CYRIC 680 AVF cyclotron, even if the injection is off-axis. The electrostatic mirror seems appropriate due to the space limitation in the central region. The injection scheme presented here with the quadrupole like electrodes for steering the particles off-axis seems a feasible option. However, more detailed studies of the shapes of the electrode as well as the puller will be needed if an actual system is to be built.

References

- 1) Honma T. et al., CYRIC Ann. Rept. (1991) p.64.
- 2) Kost C. J. and Jones F.W., RELAX3D, TRIUMF internal report TRI-88-01.
- 3) Bellomo G. et al., Nucl. Instr. and Meth., 206 (1983) p.19-46.

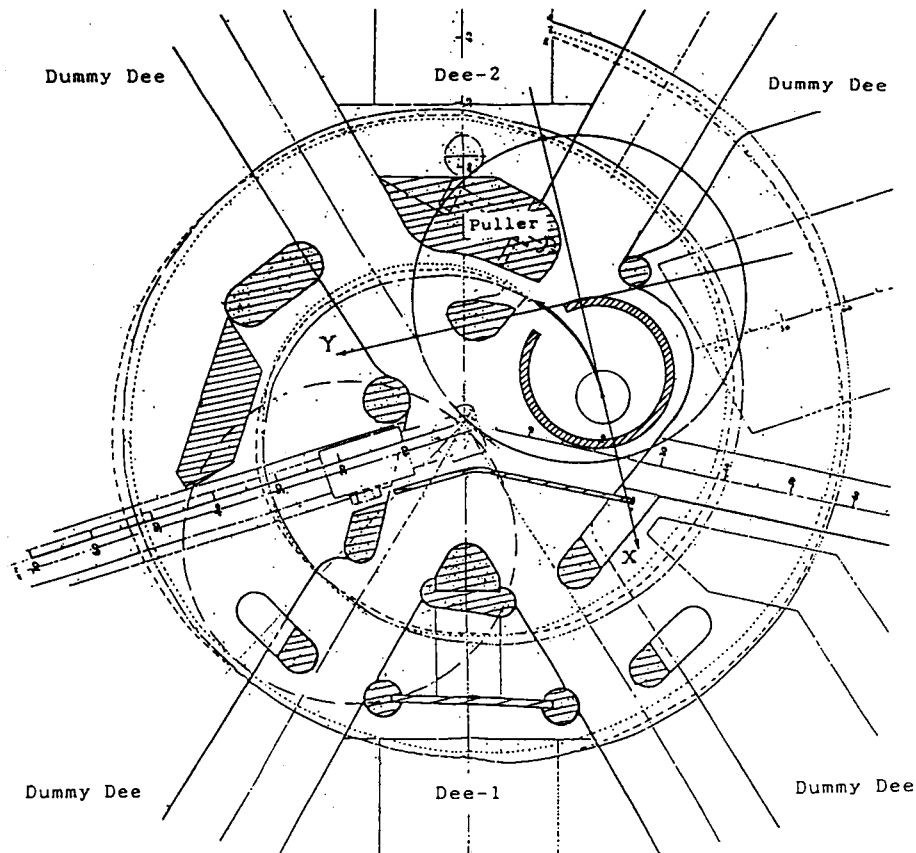


Fig. 1. Central region geometry with inflector housing of electrostatic mirror type which is positioned off-axis of 15 mm from axial hole center.

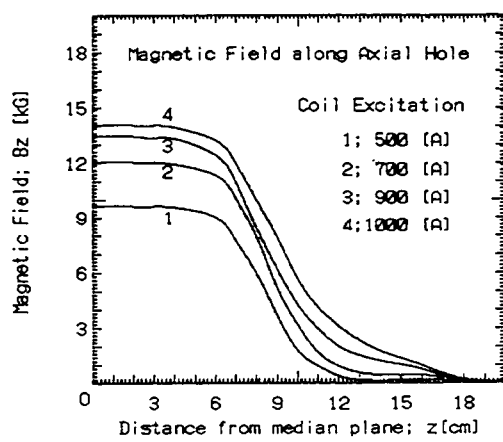


Fig. 2. Magnetic field along the axis of the cyclotron axial hole for various excitations of the main coil.

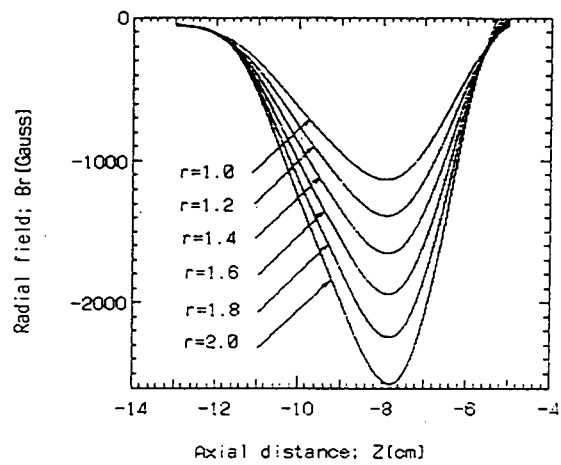


Fig. 3. Calculated radial magnetic field component $B_r(r, z)$ in the axial hole for various radii at excitation current of 500 A.

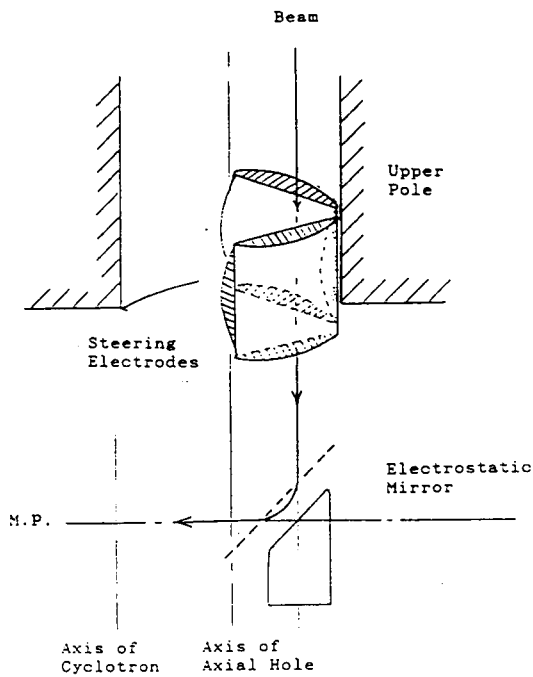


Fig. 4. Schematic drawing of steering electrode assembly in the axial hole together with electrostatic mirror type inflector.

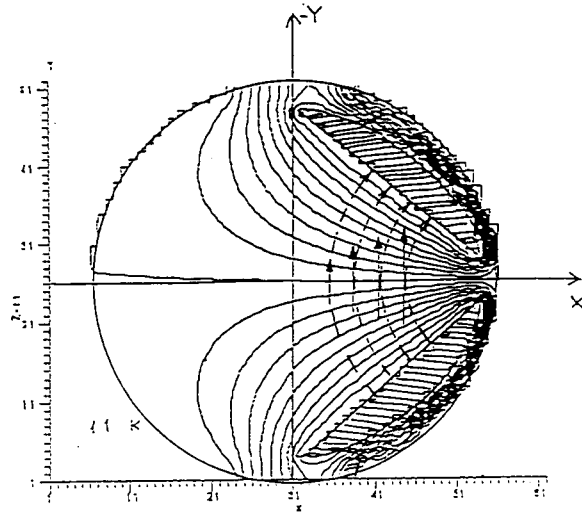


Fig. 5. Equipotential lines at $z = 8$ cm in the steering electrode assembly calculated by using RELAX3D.

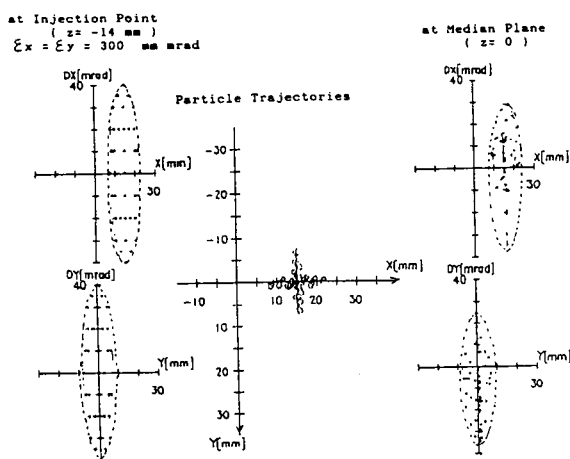


Fig. 6. Projections of particle trajectories onto the x-y median plane, and phase space plots in the (x, x') and (y, y') planes at the starting point (left) and at the cyclotron median plane (right) in reference to $x = 15$ mm off-axis ray.

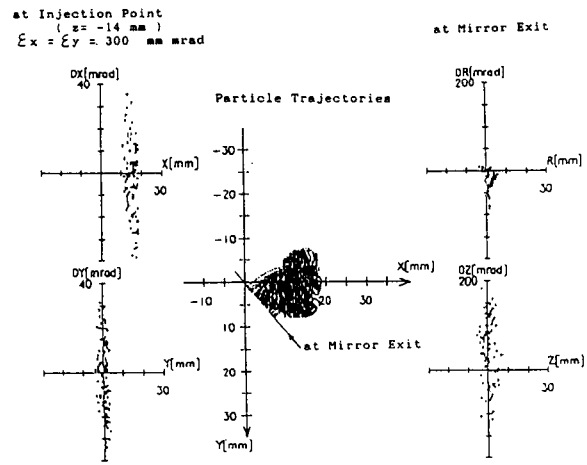


Fig. 7. Projection of particle trajectories onto the x-y median plane from the starting point to the exit of the mirror housing, and phase space plots in the both (x, x') and (y, y') at the starting point (left) and $(r, r'), (z, z')$ planes at the exit of mirror housing (right) in reference to $x = 15$ mm off-axis ray.